Dielectric Relaxation in Blends of Amorphous Poly(DL-lactic acid) and Semicrystalline Poly(L-lactic acid)

Jindong Ren and Keiichiro Adachi*

Department of Macromolecular Science, Graduate School of Science, Osaka University, Toyonaka, Osaka 560-0043, Japan

Received April 3, 2003; Revised Manuscript Received May 14, 2003

ABSTRACT: We investigated the thermal and dielectric behavior of blends consisting of semicrystalline poly(L-lactic acid) (L-87) and amorphous poly(DL-lactic acid) (DL-74 and DL-7). Two series of blends L-87/DL-74 coded as B1 and L-87/DL-7 coded as B2 were used where the code number indicates molecular weight M_w in kg/mol. The DSC thermograms of quenched blends exhibited a single glass transition at about 326 K followed by the exothermic peak due to crystallization of L-87. The relatively sharp glass transition indicates that both components are miscible in the molten state. The degree of crystallinity χ was determined from the heat of fusion. Three dielectric loss peaks were observed for B2. They are termed α_n, α_s, and β as reported previously [*Macromolecules* **2003**, *36*, 210] and are assigned to the normal mode relaxation of DL-PLA dissolved in the amorphous region, the segmental mode process, and local twisting motions of the main chains, respectively. The dielectric relaxation time for the α_n relaxation was almost independent of χ, but the distribution of relaxation times was broader than that for pure DL-PLA. The distribution of relaxation times for the α_s relaxation also broadened with increasing χ. The relaxation strength $\Delta\epsilon$ for the α_s relaxation was lower than the value expected from the linearity of $\Delta\epsilon$ against $1 - \chi$, indicating the existence of two amorphous regions A-1 and A-2. In the region A-1 the segmental motions are allowed, but in the region A-2 local segmental motions are heavily damped. The data for the α_n process indicate that the DL-PLA chains exist in the region A-1. On the other hand, the intensity of the β relaxation was not sensitive to the crystallinity, indicating that local twisting motions are not restricted, even in the region A-2.

Introduction

Recently we reported the dielectric properties of poly(DL-lactic acid) (DL-PLA) with the D/L ratio of 1/3 in the bulk and solution states.[1,2] The PLA samples were perfectly amorphous and exhibited three dielectric loss peaks designated as α_n, α_s, and β in the order of decreasing temperature. The α_n process was assigned to the normal mode relaxation due to fluctuation of the end-to-end vector.[3,4] On the other hand, the α_s and β processes were attributed to segmental motions associated with the glass transition and the local twisting motions of the chains in the glassy state, respectively. The dielectric properties of DL-PLA were also reported by Mierzwa et al. for DL-PLA.[5] Mijovic and Sy[6] studied the effect of crystallinity on the dielectric α_s relaxation in semicrystalline poly(L-lactic acid) (L-PLA) with various degree of crystallinity. They found that the crystallization does not affect the relaxation time of the α_s process in contrast to the dielectric behavior of most crystalline polymers.[7,8] The viscoelastic relaxations in L-PLA[9,10] and DL-PLA[1,5] were also reported by several authors.

PLA is a biodegradable polymer and used as an eco-friendly material.[11−13] The physical properties of PLA depend on the degree of crystallinity, and therefore the control of the crystallinity is important for practical applications of PLA. One of the methods is to mix a crystalline polymer with the atactic polymer of the same kind. For instance, it is reported that syndiotactic (st-) and atactic (at-) polystyrenes (PS) are miscible in the molten state, but in the solid state, at-PS segregates from the crystallites of st-PS.[14,15] As is well-known, semicrystalline polymers have a morphology that the lamella crystallites and the amorphous region are piled alternatively. Questions are raised: where the at-chains reside and how the dynamics of those at-chains are constrained by the crystallites. Melt-miscible blends consisting of crystalline and amorphous polymers are similar in the present system.[16,17] Runt reviewed the structure and properties of melt-miscible crystalline blends.[16] Three types of the microstructure were suggested; i.e., the amorphous component resides in the interlammela, interfibriller, and intersherulitic regions.

Motivated by those studies, we have investigated the dielectric behavior of blends of semicrystalline L-PLA and amorphous DL-PLA. It is expected that motions associated with both the α_n and α_s relaxations are constrained in the amorphous phase. Focusing our attention on the effects of the crystallites on the dynamics of the PLA chains, we studied the miscibility and dynamics in the blends of L-PLA and DL-PLA by means of differential scanning calorimetry (DSC) and dielectric relaxation spectroscopy.

Experimental Section

L-PLA was supplied from Mitsui Chemicals Co. (Tokyo, Japan). The L-PLA was purified by precipitating it from chloroform solutions in excess amount of methanol under vigorous stirring. The powderlike precipitate was dried under vacuum of 0.01 Pa at about 310 K for 5 days, and thus purified L-PLA is coded as L-87. DL-PLA was synthesized with Sn-$(C_8H_{15}O_2)_2$ as reported by Ajioka et al.[18] Details of the synthesis and characterization were reported previously.[1] We used two DL-PLA samples: DL-74 is the unfractionated sample with broad distribution, and the other DL-7 is the fractionated sample. The weight-average molecular weight M_w and the polydispersity (M_w/M_n) are listed in Table 1.

* Corresponding author. Phone/FAX +81-6-6850-5464; e-mail adachi@chem.sci.osaka-u.ac.jp.

10.1021/ma034420v CCC: $25.00
Published on Web 06/14/2003

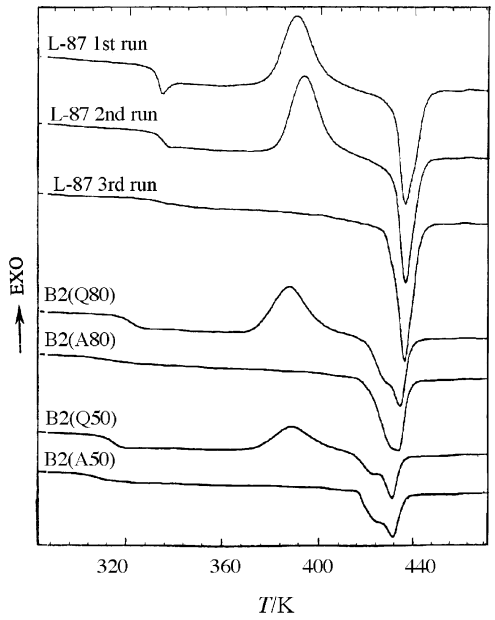

Figure 1. DSC diagrams of L-87, B2(Q80), and B2(Q50).

Table 1. Characteristics of PLA Samples

code	$10^{-3}M_w$	M_w/M_n
L-87	87	3.0
DL-74	74	3.7
DL-7	7.0	1.22

Although it was desirable to use fractionated DL-PLA throughout this study, we used both of DL-74 and DL-7 to prepare the blends because the amount of the fractionated DL-7 was not enough to prepare the blend samples varying a wide range of the compositions. Blends of L-PLA and DL-PLA were prepared by dissolving prescribed amounts of the component polymers in chloroform, and then the solutions were cast into film in an ambient atmosphere. Thus, prepared films were dried in a vacuum of 0.01 Pa at 320 K for several days. We prepared two series of the blends: L-87/DL-74 coded as B1 and L-87/DL-7 coded as B2. The blend samples are coded such as B1(A30), which indicates that the mixing ratio of L-87/DL-74 = 30/70 by weight and "A" indicates that the sample has been annealed at 420 K for 10 min for crystallization of the blend. For the quenched samples, "A" is replaced by "Q".

Dielectric measurements were carried out with an RLC bridge (QuadTech model 7600, Maynard, MA) over the frequency range from 10 Hz to 2 MHz and temperature range from 100 to 410 K. Measurements of differential scanning calorimetry (DSC) were made at the heating rate of 10 K/min by using an apparatus (Seiko SSC-580, Tokyo, Japan).

Results and Discussion

Thermal Behavior and Crystallinity. Figure 1 shows the DSC thermograms of L-87, B2(50), and B2-(80). For L-87, measurements were made as follows. First, the first run was conducted for the sample prepared as described in the Experimental Section, and then the sample was quenched from 470 K to a room temperature at a rate of about −50 K/min, and then the second run was conducted. After the measurement of second run, the sample was annealed at 420 K for 10 min; then the sample was cooled to room temperature, and the measurement of the third run was conducted.

In the first run of L-87, a small endothermic peak at the glass transition temperature T_g (= 330 K) was observed. This small peak disappeared in the second run for the quenched sample and hence can be attributed to the enthalpy relaxation. The first run indicates that L-87 precipitated from solutions is almost amorphous. An exothermic peak due to crystallization was observed around 395 K, and subsequently the endothermic peak due to melting was observed at 430 K. Comparing the melting peaks of the first and second runs, we recognize a small shoulder in the melting peak of the first run at about 445 K, but this shoulder is not seen in the second run. This indicates that there exist two crystalline modifications. We also note by comparison of the second and third runs of L-87 that T_g of the crystallized L-PLA is slightly higher than the amorphous L-PLA. The thermal behavior of B2 is essentially similar to L-87. We note that the T_g and melting peak of B2 locate slightly lower temperature than L-87. This can be explained by the lower T_g of DL-7 than L-87 due to the effects of the stereoregularity and the molecular weight.

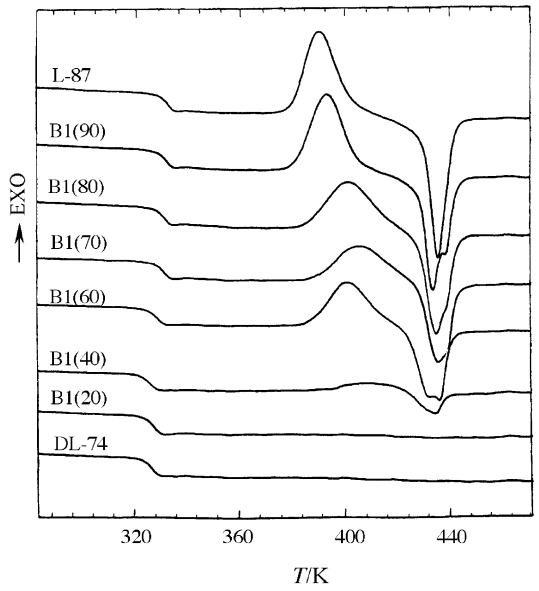

Figure 2. DSC thermograms of B1 and the components quenched from 470 K.

A systematic study on the effect of the blend composition was made for B1. Figure 2 shows the DSC thermograms of B1 quenched from 470 K to room temperature. It is seen that DL-74 does not exhibit crystallization and fusion, and hence it is perfectly amorphous as reported previously.[1] The T_g's of quenched L-87 and DL-74 are 334 and 326 K, respectively. In the blends no broadening of T_g is seen, indicating that L- and DL-PLAs are miscible in the molten state. This was also confirmed by observation of B1(A50) under a polarizing microscope at the magnification of 400: there was no indication of the macroscopic phase separation. With decreasing content of L-87, the intensity of the exothermic peak due to crystallization decreased and the peak shifted to higher temperature. At the same time, the intensity of the melting peak decreased. When the L-PLA content was less than 20%, the blends were completely amorphous and no melting peak was observed. We note that the melting peaks of B1 and B2 are also bimodal. This behavior is similar to the behavior of the st-PS/at-PS system.[16,17] However, the polymorphism in the PLA crystal is out of scope of the present paper and will be discussed elsewhere.

The degree of crystallinity of the samples was calculated from the enthalpy of fusion. Conflicting values of the enthalpy of fusion ΔH_m^0 for the perfectly crystalline PLA were reported by several authors, and it ranges

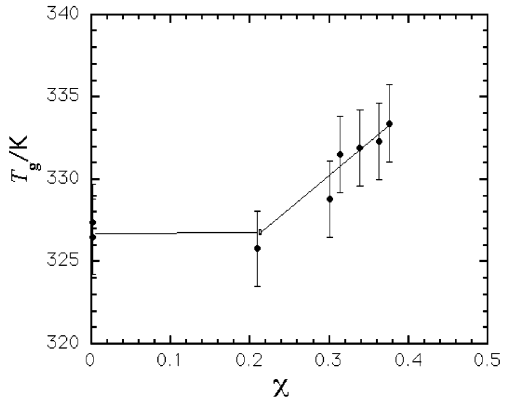

Figure 3. Dependence of T_g on the crystallinity χ.

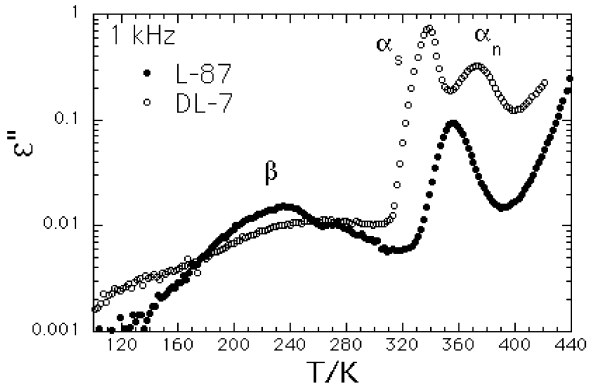

Figure 4. Comparison of ϵ'' curves at 1 kHz between L-87 annealed at 420 K and DL-7.

from of 83 to 148 J/g.[19−23] Among those data, we employed $\Delta H_m^0 = 106$ J/g reported recently by Sarasua et al.[19] and calculated the degree of crystallinity χ for B1 annealed at 420 K for 10 min. With increasing χ, T_g increased as shown in Figure 3.

Dielectric Behavior. The temperature dependence of ϵ'' for L-87 annealed at 420 K and that for DL-7 are compared in Figure 4. Three relaxation processes are observed for DL-7 in the temperature regions around 380, 340, and 250 K at 1 kHz. According to our previous dielectric study on DL-PLA,[1] those relaxation processes were assigned respectively to the normal mode α_n, the segmental mode α_s, and the secondary relaxation process β in the glassy state. For L-87 two loss peaks are seen around 360 and 230 K. Since T_g of L-87 is higher than DL-7, the peak at 360 K can be assigned to the α_s process. It is seen that the intensity for the α_s relaxation for L-87 is about 1 order lower than that for DL-7 due to the decrease of the amorphous fraction. We also recognize that the loss peaks for L-87 locate at temperatures about 15 K higher than that for DL-7 if compared at the same frequency.

In the ϵ'' curve for L-87 no α_n peak is seen. This is explained as follows. Usually melt-crystallized polymers have lamella morphology. The amorphous region between two lamellae is composed of loop chains, tie chains, and dangling chains (cilia). Among them, the loop and tie chains do not exhibit the α_n relaxation because the both ends of those subchains are fixed at the crystalline lamellae. The relaxation time for the normal mode of dangling chains (cilia chains) depends on the molecular weight M(cilia) between the free end and the end fixed at the surface of the lamella. If the Rouse model is applicable, the relaxation time is proportional to $4M(\text{cilia})^2$.[3,4] Since M(cilia) is expected to be much lower than the total molecular weight (87 000), this mode may be observed in the audio frequency range used in the present study. However, if M(cilia) is assumed to be a few thousand, the weight fraction of the M(cilia) becomes less than 5%. This is too small to be detected.

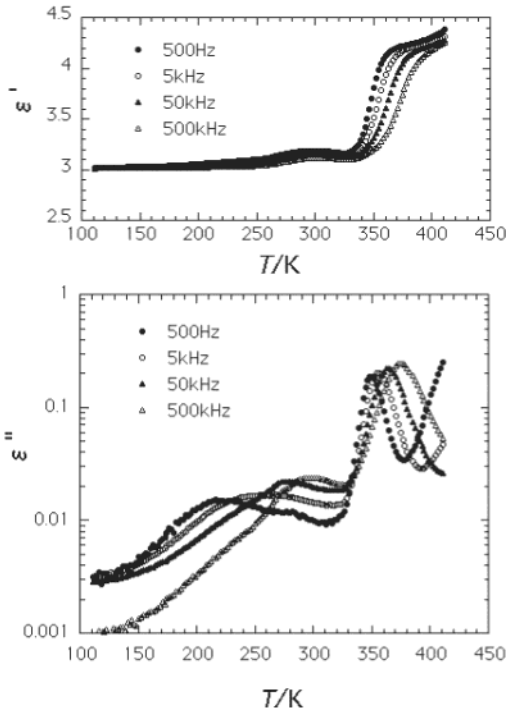

Figure 5. Temperature dependencies of ϵ' (a) and ϵ'' (b) for B1(A80).

The representative temperature dependencies of the dielectric constant ϵ' and loss factors ϵ'' for B1(A80) are shown in Figure 5. Similar behavior was observed for B1 with the other composition. We also see that the behavior is similar to pure L-87 (Figure 4). One may expect that the DL-74 chains in B1(A80) exhibit the α_n relaxation. However, this mode is not observed for two reasons. First, the loss peak for the α_n relaxation of DL-74 locates at a temperature region much higher than 370 K since the molecular weight is relatively high. Second, DL-74 exhibits a broad loss peak on account of the broad distribution of molecular weight.

Figure 6 shows the temperature dependence curves of ϵ' and log ϵ'' for B2(Q50) which has been quenched from the melt. As indicated for the DSC curves (Figure 1), the quenched blends are amorphous below T_g, but they exhibit crystallization above T_g. It is seen that ϵ' decreases steeply at about 360 K due to crystallization of L-87. The ϵ'' curves at 500 Hz and 5 kHz exhibit a steeper slope in the high-temperature side due to the crystallization. The crystallization occurred at lower temperature than the temperature observed by DSC (see Figure 2) since the heating rate in the dielectric measurement was about 0.5 K/min and was much lower than that for the DSC measurements (10 K/min).

Figure 7 shows the temperature dependence curves of ϵ' and ϵ'' of the blend B2(A50) annealed at 420 K. No crystallization occurred during the dielectric measurement, and hence the curves did not exhibit anomaly as observed for B2(Q50). Comparing Figures 6 and 7, we note that the loss peak temperature at 500 Hz for the quenched B2 is ca. 10 K higher than that for the

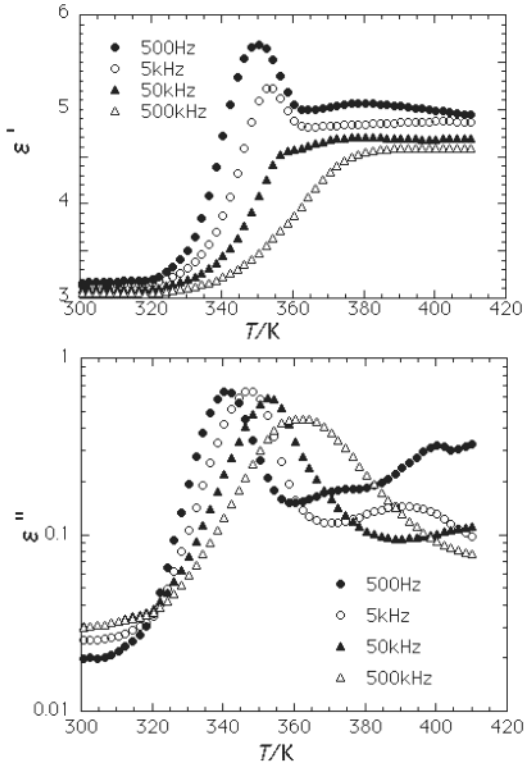

Figure 6. Temperature dependence curves of ϵ' and ϵ'' of the blend B2(Q50).

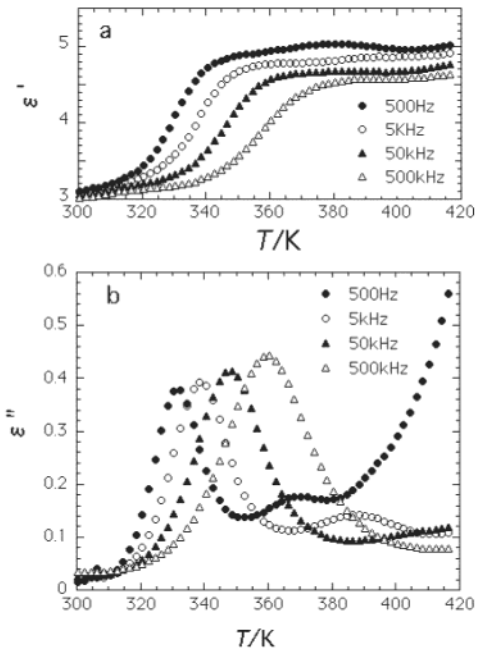

Figure 7. Temperature dependence curves of ϵ' and ϵ'' of the blend B2(A50) annealed at 420 K.

annealed B2. This can be explained by considering the effect of higher T_g of L-87 than DL-7: the content of DL-7 in the amorphous region of the crystallized blend is higher than that in the perfectly amorphous blend. The dielectric dispersion in the ϵ' curve and loss peak due to the α_n relaxation can be seen in the range from 360 to 400 K. When the content of L-87 was increased, B2(80) exhibited a very weak α_n peak.

Figure 8 shows the frequency dependencies of ϵ'' at 350 K for the α_s relaxation of B1(A) with varying contents of L-87. With increasing content of L-PLA, the

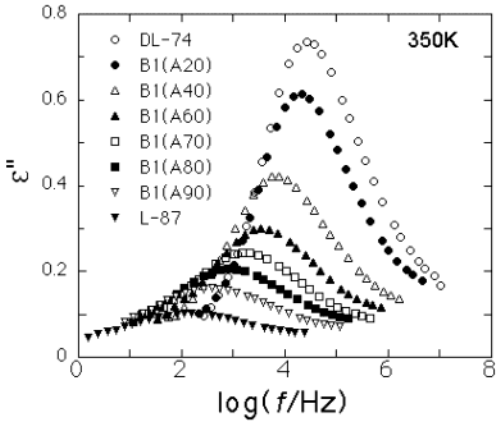

Figure 8. Frequency dependence curves of ϵ'' at 350 for B1 annealed at 420 K.

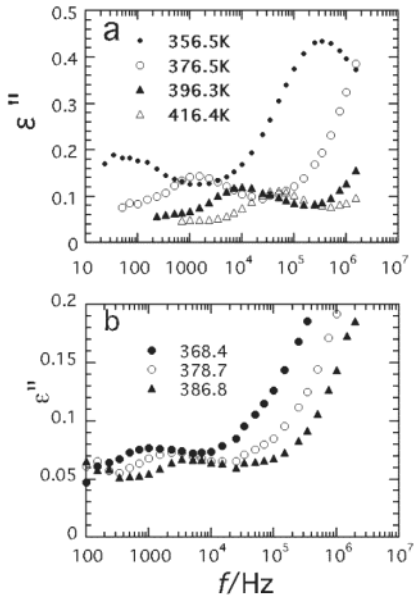

Figure 9. Frequency dependencies of ϵ'' of B2(A50) (a) and B2(A80) (b) at temperatures where the α_s and α_n relaxations are observed.

height of the ϵ'' peak decreased. Obviously, this is due to decrease of the amorphous fraction. It is seen that the loss peak shifts to lower frequency with increasing content of L-87, reflecting the higher T_g of L-87 than DL-74.

Parts a and b of Figure 9 show the frequency dependencies of ϵ'' of B2(A50) and B2(A80), respectively, at temperatures where the α_s and α_n relaxations are observed. With increasing temperature the α_s peak shifts to higher frequency, and the small peak due to the α_n process appears in our experimental window. For B2(A80) the α_n peak is very weak but is seen clearly as shown in Figure 9b.

Figure 10 shows the Arrhenius plots for the α_s and α_n relaxations where the logarithm of the loss maximum frequencies f_m are plotted against the inverse of temperature T. It is seen that the plots for the α_s relaxation shift with the composition reflecting the glass transition temperature of the blends (Figure 3). The plots conform to the Vogel−Fulcher−Tammann(VFT) equation[24,25] as observed commonly for α_s relaxations:

$$\log f_m = A - \frac{B}{T - T_0} \qquad (1)$$

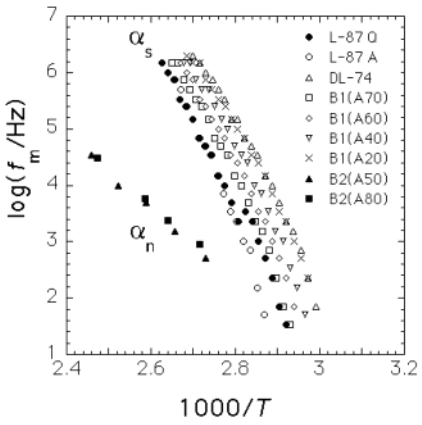

Figure 10. Arrhenius plots for the α_s and α_n relaxations.

Table 2. Parameters of the VFT Equation[a]

code	B	T_0/K	code	B	T_0/K
L-87(A)	535	300.3	B1(A60)	594	285.9
B1(A90)	548	296.4	B1(A40)	588	284.1
B1(A80)	573	292.1	B1(A20)	611	277.9
B1(A70)	575	290.2	DL-74	582	280.6

[a] $A = 12.8$ for all blends and the components.

where A, B, and T_0 are the parameters. We have fitted our data to the VFT function by assuming that A has a common value of 12.8 for all blend samples. This is because A is sensitive to a small error and changed unsystematically against the composition. The data conformed well to the VFT function with the average of those values. The parameters are listed in Table 2.

Before discussing the behavior of blends, we look at the behavior of pure L-87. In Figure 10, the data for the α_s process of quenched (Q) L-87 which were measured in the heating direction are plotted with solid circles. As mentioned above, crystallization occurs around $1000/T = 2.8$, where log f_m decreases suddenly. Above this temperature the values of log f_m coincide with those for annealed L-87. This indicates that the amorphous L-87 prepared by quenching exhibits slightly higher f_m than crystalline L-87 and is not in harmony with the result reported by Mijovic and Sy,[12] who reported that crystallization of L-PLA did not affect the peak frequency. In Table 2, we see that T_0 decreases with increasing content of DL-74 mainly due to the difference of T_0 between L-87 and DL-74.

It is seen that the loss maximum frequencies f_m for the α_n relaxation in B2(A50) and B2(A80) are almost the same as that of pure DL-7. This behavior is contrary to our expectation and suggests that the size of the amorphous region in the blends is larger than the end-to-end distance of the DL-7 chains, and hence the constraint against the normal mode process is weak as discussed later.

Distribution of Relaxation Times. The normalized dielectric loss curves for the α_s relaxation of B1(A), annealed L-87, and DL-74 are compared in Figure 11, where we see that the ϵ'' curve broadens with increasing content of L-87. Although not shown here, quenched L-87 exhibited the narrow ϵ'' curve similar to DL-74. This behavior is common to semicrystalline polymers such as poly(ethylene telephthalate) and poly(carbonate) that the distribution of relaxation times in a semicrystalline state is broader than that in the perfectly amorphous state.[26] The data reported by Mijovic and Sy also indicate that the loss curve broadens with

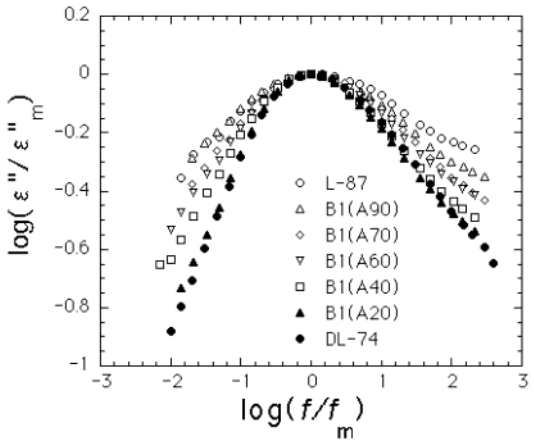

Figure 11. Normalized ϵ'' curves for the α_s relaxation of B1-(A), annealed L-87, and DL-74.

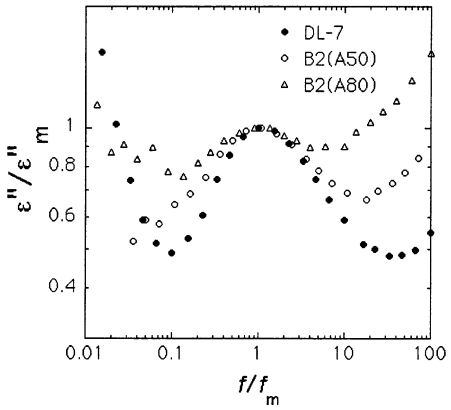

Figure 12. Normalized ϵ'' curves for the α_n relaxation of B2-(A) and DL-7.

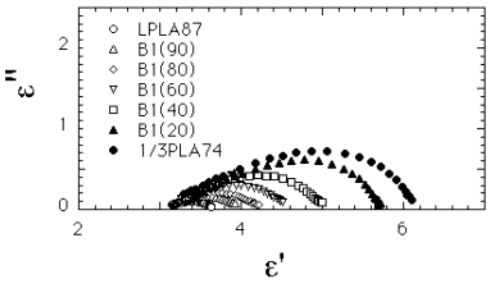

Figure 13. Cole−Cole plots for B1.

increasing degree of crystallinity.[6] The segmental motions in the amorphous region are subjected to a variety of constraints imposed by the crystallites.

Figure 12 shows the normalized ϵ'' curves for the α_n process of pure DL-7, B2(A50), and B2(A80). It is seen that the loss curves of B2(A50) and B2(A80) are broader than that of DL-7, and the extent of broadening increases with the content of L-87. This result indicates that the crystallites of L-87 affects the distribution of relaxation times although the average relaxation time is almost independent of the crystallinity.

Relaxation Strength. The relaxation strength $\Delta\epsilon_s$ for the α_s process is determined from the Cole−Cole (Figure 13) and listed in Table 3. The dependence of $\Delta\epsilon_s$ on the degree of the crystallinity χ is shown in Figure 14. We see that $\Delta\epsilon_s$ is not linear with respect to χ, and it decreases steeply around $\chi = 0.3$. The simplest model of semicrystalline polymers assumes the coexistence of

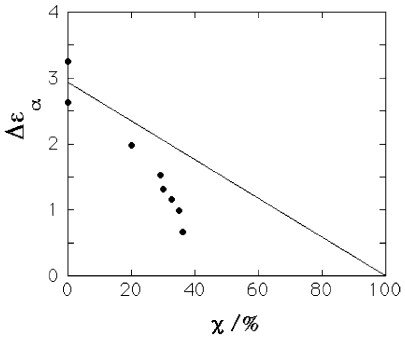

Figure 14. Relaxation strength $\Delta\epsilon_s$ for the α_s process vs crystallinity χ.

Table 3. Heat of Fusion ΔH_m, Crystallinity χ, and Relaxation Strength $\Delta\epsilon_s$ for the α_s Process

code	ΔH_m/J g^{-1}	χ/%	$\Delta\epsilon_s$
L-87	39.8	36.1	0.63
B1(A90)	38.5	34.9	1.05
B1(A80)	35.9	32.6	1.25
B1(A70)	33.2	30.1	1.40
B1(A60)	31.9	29	1.57
B1(A40)	22.2	20.1	2.00
B1(A20)	0	0	2.50
DL-74	0	0	3.25
B2(A80)	34.4	31.2	1.44
B2(A50)	19.4	17.6	1.85

crystallites and amorphous regions having properties similar to the pure amorphous state. Obviously, this model predicts $\Delta\epsilon_s$ is linear against χ. The data shown in Figure 14 do not agree with this simple expectation, indicating the existence of the interphase where segmental motions are suppressed. Here we note that although the crystallinity of B1(A20) is zero, its $\Delta\epsilon_s$ is lower than DL-74 beyond the experimental error, as shown in Figure 13. We speculate that the nuclei of the L-PLA crystal are formed, and there exists the interphase around the nuclei.

The relaxation strength $\Delta\epsilon_n$ for the α_n relaxation was also determined from the Cole−Cole plots to be 0.52 ± 0.05 for B2(A50) and 0.24 ± 0.05 for B2(A80) at 378 K. The values of the $\Delta\epsilon_n$ divided by concentration of DL-7 become 1.1−1.2 and is close to the value of $\Delta\epsilon_n = 1.02$ at 377 K for pure DL-7. This indicates that global motions associated with the fluctuation of the end-to-end vector of DL-7 are not strongly constrained in those blends. This is consistent with the result that the average relaxation time for the normal mode does not change by blending with L-PLA. It is reported that L-PLA and D-PLA form a stereocomplex.[27,28] The above results rule out the possibility that L-87 and DL-7 form a complex.

***β* Relaxation.** In our previous work for the β relaxation[1] of DL-PLA samples, we attributed the β relaxation to twisting motions of the main chain. The analyses of the data indicated that the amplitude of the twisting motions to be 11 degrees.[1] Figure 15 shows ϵ'' vs $1/T$ plots in the β relaxation region. Although the data scatter, the intensity tends to decrease with increasing the degree of crystallinity of the samples, indicating that the β relaxation also has its origin in the amorphous region. The area of the loss peak of the ϵ'' vs $1/T$ plot is proportional to the relaxation strength $\Delta\epsilon_\beta$. We see that $\Delta\epsilon_\beta$ does not change much with χ. This behavior contrasts to the behavior of the α_s relaxation shown in Figure 14. This indicates that the β relaxation is active in the interphase as discussed in the following section.

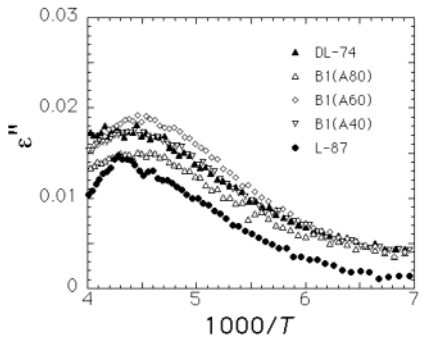

Figure 15. ϵ'' vs $1/T$ plots in the β relaxation region.

Morphology of the Blends. In this section we consider the morphology of the blends. The studies of small-angle X-ray scattering (SAXS) for poly(L-lactide-*co*-meso-lactide) containing 0−12% of DL-lactide were reported by Huang et al.[29] They reported that the long spacing L in the blend is 18−23 nm and increases with the content of DL-PLA. Chen et al.[30] reported the SAXS study on miscible blends of L-PLA and poly(4-vinylphenol). Their data indicate that $L = 22$ nm for the blend containing 20% of poly(4-vinylphenol). Those data indicate that L of the present blends is longer than 20 nm. Here we may assume that the crystalline lamellae and the amorphous layers are stacked alternatively in the present blends, and the thickness of the amorphous layer L_a is given by $(1 - \chi)L$, where χ is the volume fraction of the crystal phase. Since the crystallinity of B1 and B2 is less than 40%, L_a is 11−14 nm.

We consider whether the DL-7 and DL-74 chains can be accommodated in the interlamella region. This is judged from the relative size of the DL-PLA chains with respect to L_a. As is well-known, the dimension of a polymer chain is expressed by the characteristic ratio C_∞ and the number of the bonds. Since the monomeric unit of the PLA chains can be regarded as virtual bonds, the mean-square radius of gyration $\langle s^2\rangle$ of the PLA chains is defined by $C_\infty N b_v^2/6$, where b_v is the length of the virtual bond and N the degree of polymerization. So far, several data of C_∞ for PLA chains were reported: $C_\infty = 2.05$ by Brant et al.,[31] $C_\infty = 5.39$ by Joziasse et al.,[32] and $C_\infty = 3.15$ by Ren et al.[1] With those values, $\langle s^2\rangle^{1/2}$ of DL-7 and DL-74 become 2.1−3.4 and 6.9−11.1 nm, respectively. From these data we expect that the DL-7 chains can reside in the amorphous region without distortion of the conformation. On the other hand, the dimension of the DL-74 chains is similar to L_a and may be accommodated in the amorphous region accompanied by the distortion of the conformation of the DL-74 chains and expansion of the amorphous region.

Looking at the experimental results for the dependence of the relaxation strength for the α_s process on the crystallinity χ (Figure 14), we conclude that the amorphous region of the blends consists of regions A-1and A-2, as illustrated schematically in Figure 16. In the region A-1, the segmental motions are allowed, but in the region A-2 near the crystalline lamellae segmental motions are suppressed. The data of the distribution of the relaxation times for the α_s process (Figure 11) indicate that the boundary between the regions A-1and A-2 is not clear, and the segmental mobility varies gradually between those two regions. The thickness of the A-1 region is estimated to be about 5 nm for B1(A80) from the crystallinity and the relaxation strengths $\Delta\alpha_s$ for DL-74 and L-87. The data for

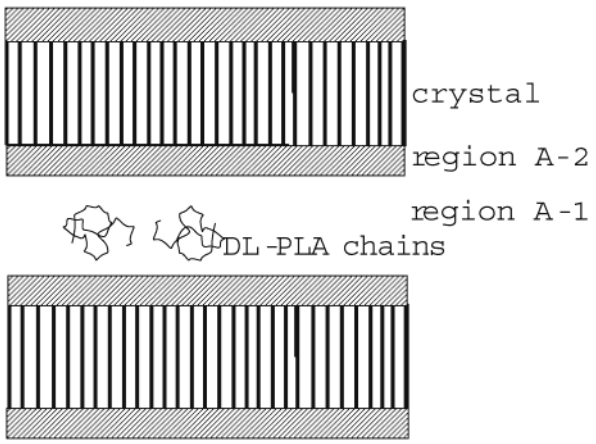

Figure 16. Morphology of L-PLA/DL-PLA blends.

B2(A50) and B2(A80) have indicated that the average relaxation time and the relaxation strength per chain for the α_n process of DL-7 did not change much from those of pure DL-7. This indicates that the motions of the DL-7 chains are not affected by the crystallites, and the DL-7 chains reside mostly in the region A-1 as depicted in Figure 16. Some DL-7 chains locate in the region A-2, and the distribution of relaxation times broadens with increasing content of L-87 as shown in Figure 12.

There is a possibility that the morphology of B1 might be different from that of B2. The present blend is similar to blends of a diblock copolymers AB and the homopolymer A. If the molecular weight of A is lower than that of the block A, the homopolymer A resides in the microdomain A of the block copolymer accompanied by the morphological transition.[33,34] The present dielectric and DSC data on B1 did not indicate any evidences of the macroscopic phase separation of DL-74 and L-87. This suggests that B1 also has the morphology as represented by Figure 16.

Conclusion

We have reported the DSC thermograms and dielectric relaxations in two series of blends B1 and B2 consisting of semicrystalline poly(L-lactic acid) (L-87) and amorphous poly(DL-lactic acid) (DL-74 and DL-7) where the code number indicates the molecular weight in kg/mol. The DSC thermograms indicate that the quenched blends exhibit a single glass transition, indicating that the components are miscible in the molten state. The crystallization of L-87 occurs above the T_g. Three dielectric loss peaks termed as α_n, α_s, and β have been observed for the crystallized blends, and they are assigned to the normal mode, segmental mode, and the secondary relaxation processes, respectively. On account of the constraints by the crystallites, the distribution of relaxation times for both the α_s and α_n processes broadens with increasing degree of crystallinity χ. The average relaxation time for the α_s decreased with increasing content of DL-PLA, reflecting the difference in T_g of the L- and DL-PLAs. The relaxation strength for the α_s relaxation is not proportional to χ and becomes almost zero at $\chi = 50\%$. Those results suggest that there are two kinds of amorphous region: the region where segmental mode is active (A-1) and the interphase (A-2) where segmental motions are heavily damped. The data for the α_n process indicate that the DL-PLA chains locate mostly in the A-1 region. If we assume a morphology that the lamella crystallites and amorphous layers are piled alternatively, the thickness of the A-1 layer becomes ca. 5 nm. The consideration on the dimension of the DL-7 chains supports this structure. On the other hand, the intensity of the β relaxation does not decrease steeply with χ, indicating that the secondary relaxation is active even in the interphase.

Acknowledgment. J.R. thanks the Ministry of Education, Culture, Sports, Science, and Technology of Japan for a scholarship.

References and Notes

(1) Ren, J.; Urakawa, O.; Adachi, K. *Macromolecules* **2003**, *36*, 210.
(2) Ren, J.; Urakawa, O.; Adachi, K. *Polymer* **2003**, *44*, 847.
(3) Stockmayer, W. H. *Pure Appl. Chem.***1967**, *15*, 539.
(4) Adachi, K.; Kotaka, T. *Prog. Polym. Sci.***1993**, *18*, 585.
(5) Mierzwa, M.; Floudas, G.; Dorgan, J.; Knauss, D.; Wegner, J. *J. Non-Cryst. Solids* **2002**, *307*, 296.
(6) Mijovic, J; Sy, J. W. *Macromolecules* **2002**, *35*, 6370.
(7) Schartel, B.; Volland, C.; Li, Y. X.; Wendorff, J. W.; Kissel, T. *J. Microencapsulation* **1997**, *14*, 475.
(8) McCrum, N. G.; Read, B. E.; Williams, G. *Anelastic and Dielectric Effects in Polymeric Solids*; Wiley: New York, 1967.
(9) Boyd, R. H.; Liu, F. In *Dielectric Spectroscopy of Semicrystalline Polymers* in *Dielectric Spectroscopy of Polymeric Materials*; Runt, J. P., Fitzgerald, J. J., Eds.; American Chemical Society: Washington, DC, 1997; Chater 4.
(10) Palade, L. I.; Lehermeier, H. J.; Dorgan, J. R. *Macromolecules* **2001**, *34*, 1384.
(11) Sinclair, R. G. *J. Macromol. Sci., Pure Appl. Chem.* **1996**, *A33*, 585.
(12) Okada, M. *Prog. Polym. Sci.* **2002**, *27*, 87.
(13) Hausberger, A. D.; Deluca, P. P. *J. Pharmaceut. Biomed.* **1995**, *13*, 747.
(14) Chiu, F. C.; Peng, C. G. *Polymer* **2002**, *43*, 4879.
(15) Woo, E. M.; Sun, Y. S.; Yang, C. P. *Prog. Polym. Sci.* **2001**, *26*, 945.
(16) Runt, J. P. In *Dielectric Studies of Polymer Blends* in *Dielectric Spectroscopy of Polymeric Materials*; Runt, J. P., Fitzgerald, J. J., Eds.; American Chemical Society: Washington, DC, 1997; Chapter 10.
(17) Crevecoeur, G.; Groeninckx, G. *Macromolecules* **1991**, *24*, 1190.
(18) Ajioka, M.; Enomoto, K.; Suzuki, K.; Yamaguchi, A. *Bull. Chem. Soc. Jpn.* **1995**, *68*, 2125.
(19) Sarasua, J. R.; Prudhomme, R. E.; Wisniewski, M.; Borgne, A. L.; Spassky, N. *Macromolecules* **1998**, *31*, 3895.
(20) Fischer, E. W.; Sterzel, F.; Wegner, H. J. *Kolloid Z. Z. Polym.* **1973**, *251*, 980.
(21) Kalb, B.; Pennings, A. J. *Polymer* **1980**, *21*, 607.
(22) Cohn, D.; Younes, H.; Marom, G. *Polymer* **1987**, *28*, 2018.
(23) Gilding, D. K.; Reed, A. M. *Polymer* **1979**, *20*, 1459.
(24) Vogel, H. *Phys. Z.* **1921**, *22*, 645.
(25) Fulcher, G. A. *J. Am. Ceram. Soc.* **1925**, *8*, 339.
(26) Ishida, Y.; Yamafuji, K.; Ito, H.; Takayanagi, M. *Kolloid Z.* **1962**, *180*, 108.
(27) Ikada, Y.; Jamahidi, K.; Tsuji, H.; Hyon, S.-H. *Macromolecules* **1987**, *20*, 904.
(28) Tsuji, H.; Ikada, Y. *Macromolecules* **1992**, *25*, 5719.
(29) Huang, J.; Lisowski, M. S.; Runt, J; Hall, E. S.; Kean, R. T.; Buehler, N.; Lin, J. S. *Macromolecules* **1998**, *31*, 2593.
(30) Chen, H.-L.; Liu, H.-H.; Lin, J. S. *Macromolecules* **2000**, *33*, 4856.
(31) Brant, D. A.; Tonelli, A. E.; Flory, P. J. *Macromolecules* **1969**, *2*, 228.
(32) Joziasse, C. A.; Veenstra, H.; Grijpma, D. W.; Penning, A. *J. Macromol. Chem., Phys.* **1996**, *197*, 2219.
(33) Tanaka, H.; Hasegawa, H.; Hashimoto, T. *Macromolecules* **1991**, *24*, 240.
(34) Hashimoto, T.; Tanaka, H.; Hasegawa, H. *Macromolecules* **1990**, *23*, 4378.

MA034420V